The Measurement of Doppler Wind Fields with Fast Scanning Radars: Signal Processing Techniques

JOHN R. ANDERSON*

Department of Atmospheric Sciences, University of Illinois, Urbana, IL

(Manuscript received 5 August 1986, in final form 9 April 1987)

ABSTRACT

This paper discusses signal processing techniques being developed for making Doppler wind velocity measurements using airport surveillance radars. Techniques are presented and evaluated for velocity estimation using fast-rotating radars. In addition to their fast rotation rates airport surveillance radars employ block-staggered pulse repetition rates to enhance their detection of aircraft. The effect of this transmission strategy on the weather processor clutter filter is examined. The performance of the proposed algorithms are examined as a function of the weather signal spectral width and the ground clutter/weather signal ratio.

1. Introduction

The measurement of radial wind fields by Doppler radar techniques is now a well-established practice, and radar systems incorporating various signal processing algorithms have been successfully demonstrated (Doviak and Zrnić, 1984). However, prior to this work, the developers of these algorithms have concentrated on specialized weather radar systems which have relatively slow scanning rates and consequently a large number of radar pulses per effective scanning beamwidth. Here we will present a design study which starts from a somewhat different set of goals. Our major objective is to evaluate the potential of Airport Surveillance Radars (ASRs) to measure wind field parameters with sufficient accuracy to detect events such as the outflows associated with strong thunderstorm downdrafts and the wind field signatures of thunderstorm gustfronts. This work differs from previous Doppler radar studies in several respects due to the major differences between the fast-scanning ASRs and conventional weather radars.

The ASR differs from conventional weather radars in many respects. For our purposes, one of the most important parameters is the very fast antenna rotation rate (approximately 13 RPM). This rotation rate is necessary for the radar to perform its primary role: observing aircraft traffic near an airport. However, the resultant small number of pulses per beamwidth poses a serious complication when making wind velocity measurements in the presence of ground clutter. This situation is aggravated by the use of a block-staggered radar Pulse Repetition Frequency (PRF) to remove aircraft Doppler velocity ambiguities. The transmitted waveform of the most modern ASR, the ASR-9, consists of a ten-pulse Coherent Processing Interval (CPI) at the higher PRF followed by an eight-pulse CPI at a lower PRF.

The target channel of the ASR-9 radar is instrumented to a maximum range of 111 km (60 nmi.) and has a mean unambiguous Doppler velocity interval of -30 to $+30$ m s^{-1} which corresponds to a mean radar carrier frequency of 2800 MHz and a mean pulse repetition interval of 1/1100 s. A more detailed description of the ASR-9 radar is given by Taylor and Brunins (1985).

In this paper we will concentrate on the development of new algorithms for achieving our signal processing goals. Particular emphasis has been placed on the performance of these algorithms in the presence of large ground clutter echoes since much of the region of interest lies at short ranges. A second major concern regarding the use of ASR-type radars for wind field measurements is related to the vertical beam profile of the radar, which is quite broad. We will not address that topic in this paper; however, we do expect that the useful range of the radar when processing weather echoes will be substantially less than the target channel, perhaps 15 km. The useful range of the Doppler weather products is limited by the contamination of low-altitude weather velocity data by higher-altitude echoes associated with larger radar reflectivities.

A field observing program is planned in order to more fully explore this issue. The results of this field study will be part of a separate analysis of the effects of the vertical beamshape which should be completed in the near future.

* Current Address: Department of Meteorology, University of Wisconsin-Madison, WI 53706.

2. System configuration and evaluation methods

The part of the radar system with which we will concern ourselves is the processing, which starts with the digitized in-phase and quadrature video and ends with the output of a radial wind velocity measurement. The processing consists of three basic elements.

The first element is a clutter rejection filter designed as a bandpass filter with a notch near zero frequency. For this analysis, we will use a linear finite-impulse response (FIR) filter designed using conventional design techniques.

The second element of the system is the actual weather velocity estimation algorithm. Much work has been performed on this topic in recent years. A discussion of velocity estimator performance is given by Shirakawa and Zrnić (1983). Here we will examine two candidate algorithms: a standard pulse pair autocorrelation method and an algorithm utilizing an oversampled filter bank. The two processors represent different estimation strategies. The autocorrelation estimator is designed based on considerations regarding the estimation of the mean frequency of a random process with no explicit consideration of clutter. When used with the pulse pair processor, the role of the clutter rejection filter is to remove the ground clutter echo as completely as possible with as little damage as possible to the weather echo. The departure point for the filter bank estimator is the realization that the effects of the fast-scanning antenna beam preclude the complete elimination of the ground clutter without a major impact on the low-velocity weather echoes. The filter bank processor takes advantage of the fact that it is possible to measure high-velocity weather echoes even in the presence of very large clutter amplitudes (clutter/signal ratios of 50 dB or greater); however, it only attempts the detection of lower velocity weather at more favorable signal-to-clutter ratios. An assessment of the performance of this class of estimator has been recently presented by Hardesty (1986).

The final element of the processing system is an incoherent averaging process which integrates over time from scan to scan. In this study, we will take the averaging time to be 6 scans. This corresponds to about 27 seconds for the ASR-9, thus the results of this study could be compared with the performance of a standard weather radar operating at 2 RPM in that both would have a similar total dwell time per antenna beamwidth. For the purposes of this study, we have assumed that the length of the scan period is adequate to completely decorrelate the trials which enter into this averaging process.

The test signals which will be used to evaluate the processing scheme are synthetically constructed complex time series that are designed to emulate the statistical properties of actual weather and clutter echoes. A discussion of the generation of such series is given in Zrnić (1975). In this study synthetic time series for both the weather and clutter echoes are generated by taking a randomly generated normal process of the appropriate amplitude and passing it through a long (200-point) FIR filter whose frequency response is a good approximation to a Gaussian power spectrum with the appropriate parameters.

The simulated ground clutter series was constructed with the center of the filter frequency response at zero velocity and the width of the filter commensurate with the modulation of stationary clutter by a Gaussian antenna beam with azimuth beamwidth of 1.4 degrees, and rotation rate of 13 RPM corresponding to an ASR-9. The mean velocity and intrinsic weather spectral width are parameters defined for each trial and include the spectral broadening effects of the antenna rotation (Atlas, 1964). Calculations have been made for intrinsic weather spectral widths of 0, 2 and 4 m s^{-1}. Values of the time series are generated at a sample interval of 1/4.5 times the mean pulse repetition interval (PRI) so that the effects of the block stagger can be simulated by taking every fifth sample for the slow PRF CPI and every fourth sample for the fast PRF CPI. Most of the cases in which we are interested are limited by clutter considerations rather than system noise due to the short useful range of the radar for wind measurements. In this light we have not included any white noise component in the synthetic signals. We have assessed the effect of including a system noise component in this analysis and find that this analysis is generally valid for clutter/noise ratios of greater than 40 dB. At lower clutter/noise ratios the removal of the noise and weather signals near zero velocity introduces an estimator bias toward the Nyquist velocity.

The actual analysis of the signal processing system is then performed using a Monte Carlo approach. Several experiments were conducted for particular choices of weather spectral widths and signal to clutter ratios. For each choice of these parameters, many trials are conducted with a range of weather velocities covering the unambiguous velocity range. For each weather mean velocity, 108 trials are conducted. The arithmetic mean of these trials is used to compute the bias, and the estimator standard deviations are computed from the 18 six-trial velocity averages which represent the incoherent integration process described above. These results are then plotted as a function of true weather velocity to indicate the estimated performance of the proposed algorithms at a specific clutter to signal ratio. Each group of 108 trials includes 54 trials of the 10-pulse high PRF cases and 54 trials of the 8-pulse low PRF cases. All of the results are computed in terms of a fraction of the Nyquist velocity, the composite plots are then scaled to velocity through the use of the Nyquist velocity associated with the mean PRI.

3. Clutter filtering techniques

The block-staggered PRF presents a fairly serious problem for the selective removal of ground clutter

echoes from the weather radar return. Ideally, one would employ a filter which has a narrow stop band notch matched to the width of the antenna modulation spectrum. In practice, this cannot be achieved if the filter processing is confined to the 8 or 10 pulses contained in one CPI since the effective beam transit time is considerably longer than the CPI. To overcome this difficulty we have adopted the somewhat unconventional technique of using a linear FIR filter across the CPI stagger boundary. Specifically, we filter each CPI using a 17 point FIR filter where the points used as input to the filter come from the CPI preceding and following as well as the desired CPI. The use of 17 points allows the calculation of the velocity estimate for any CPI by using only the information contained in that and the two adjacent CPIs. This processor can be written in the following form:

$$f_j = \sum_{k=-8}^{8} v_{j-k} h_k^0, \tag{1}$$

where h_k^0 is the filter impulse response, the v_j are the (complex) input voltage samples, and the f_j are the filtered outputs.

The output of this processor for the target CPI is then used as the input to the velocity estimation phase and the entire process is repeated one CPI later. Due to the need to have points from the following CPI, the actual velocity estimation in a real time system would be performed from delayed data one CPI behind the current antenna position, however, this should pose few practical problems.

The filter which we have used for this study was designed as a constant sample rate filter matched to the antenna spectrum for the mean PRF using the window techniques described in Oppenheim and Schaffer (1975). The filter was generated by using a Hamming window inverse transform of a notch wide enough to attenuate the antenna spectrum by 45 dB. The same coefficients are then applied to the block-staggered data which results in a filter whose frequency response varies with the position within the CPI. The window design technique was chosen due to our finding that the filters tended to degrade less when used with the block stagger than filters designed using Tchebyschev optimal techniques. A frequency response plot of the filter used in this work for a fixed radar PRF is given as the solid curve in Fig. 1. When used with the block stagger, the filter is no longer time invariant, therefore we will define a time-averaged frequency response over the target CPI which is given by

$$P(\omega) = \frac{1}{M} \sum_{j=1}^{M} \left| \sum_{k=-8}^{8} h_k^0 e^{i\omega t(j-k)} \right|^2, \tag{2}$$

where M is the number of pulses (either 8 or 10) in the target CPI and $t(j-k)$ is the time of pulse $j-k$. A plot of this time-averaged frequency response for M = 10 is given as the dashed curve in Fig. 1. The response for the M = 8 CPI is nearly identical. The attenuation of antenna-modulated zero intrinsic-width ground clutter by the block-staggered filter is 43 dB.

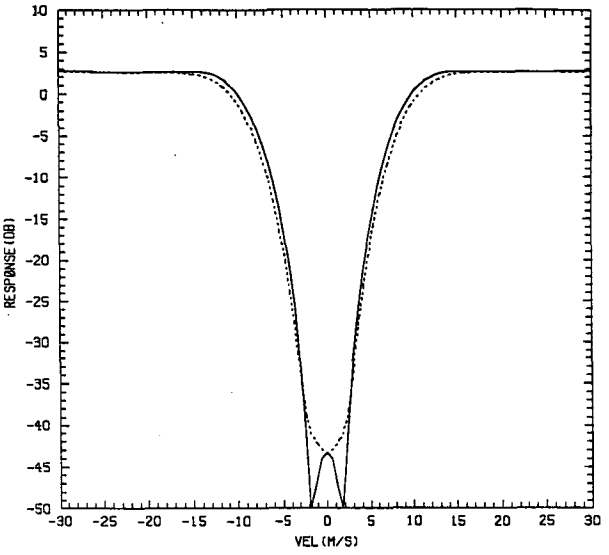

FIG. 1. The frequency response of the FIR clutter filter which is used as the first stage in the processor. The solid line is the fixed PRF response while the dashed line represents the time averaged response when used with the block-stagger radar waveform.

In order to estimate the effects of the clutter filter on the weather spectrum before we resort to the Monte Carlo simulation, we have performed a frequency domain analysis using the time-averaged response described above. The results of this analysis are presented in Fig. 2 which depicts the weather signal attenuation and velocity estimate bias for intrinsic spectral widths (spectral standard deviations) of 0, 2 and 4 m s^{-1} as a function of weather mean velocity. For the computation of the bias we have used the frequency domain analogue of the pulse pair estimator as reported by Passarelli and Siggia (1981):

$$\hat{V} = \frac{V_0}{\pi} \mathrm{Arg}\left[\int_{-\pi}^{\pi} P(\omega) S(\omega) e^{i\omega t} d\omega \right], \tag{3}$$

where V_0 is the radar Nyquist velocity, S is the weather power spectrum and $\hat{V}$ is the velocity estimate. As one can see from the figure the major effect of the filter alone is the tendency for the estimates to be biased toward the Nyquist velocity when the part of the weather spectrum near zero velocity is removed by the filter.

We have made no attempt to design the filter in such a way that it is matched to the block stagger. We do, however, plan to consider such an option in the future where different filter coefficients will be used for each pulse location in the CPI and the performance of the filter shown here should be considered a lower limit to what might be achieved as a result of such an effort.

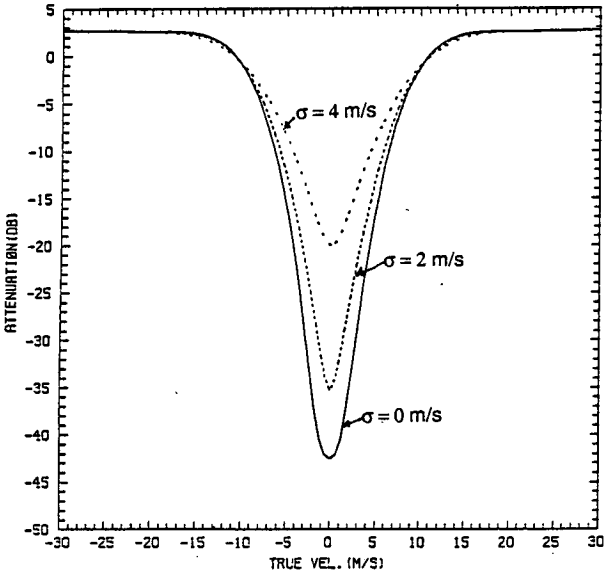

FIG. 2a. Estimated clutter filter attenuation of a Gaussian weather signal as a function of mean velocity for intrinsic weather spectral widths of 0, 2 and 4 m s^{-1}.

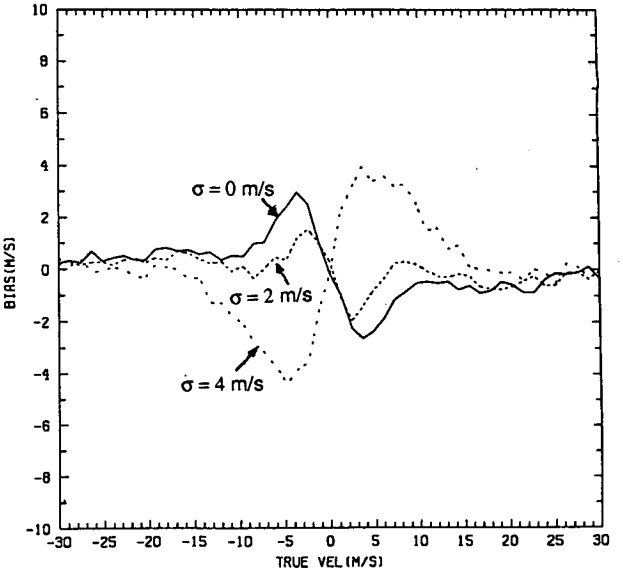

FIG. 3a. The arithmetic mean estimator bias for the clutter filter–pulse pair processor system. The figure represents the results of a Monte Carlo simulation of the processor for a clutter/signal ratio of 30 dB with the same weather parameters as Fig. 2.

4. Pulse pair velocity estimation

The first velocity estimation technique which we will consider consists of a simple autocorrelation processor applied to the target CPI after the clutter filtering. The use of this method for calculating weather mean velocities has become very common. The frequency estimate, $\hat{V}$ is given by

$$\hat{V}=\frac{V_0}{\pi}\arg\Big[\sum_{j=1}^{M-1} f_j f_{j+1}^{*}\Big]. \tag{4}$$

We will evaluate the performance of this algorithm for several signal/clutter ratios using the Monte Carlo method. In Figs. 3 and 4, we will examine the performance of this estimator for clutter/signal ratios of 30 and 40 dB including the six-trial incoherent integration process. As one might expect from the use of a clutter filter with 43 dB of clutter rejection, the six sample average weather velocity estimates begin to show a sig-

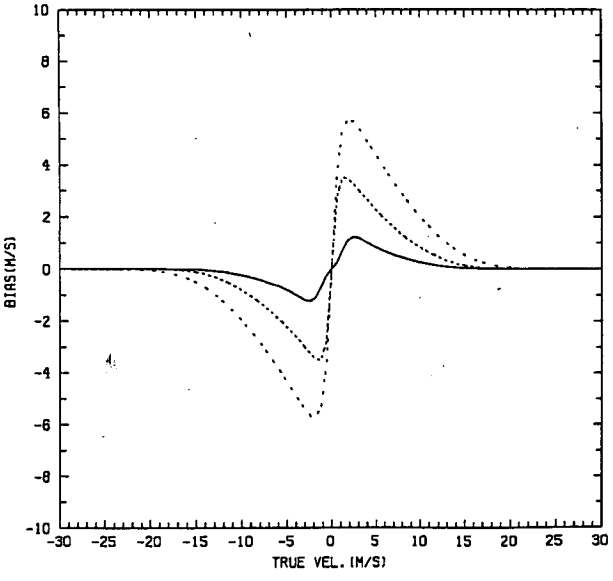

FIG. 2b. Estimated clutter filter induced velocity bias for the same weather cases as shown in Fig. 2a. The method of calculating bias is equivalent to a pulse pair velocity estimator (see text).

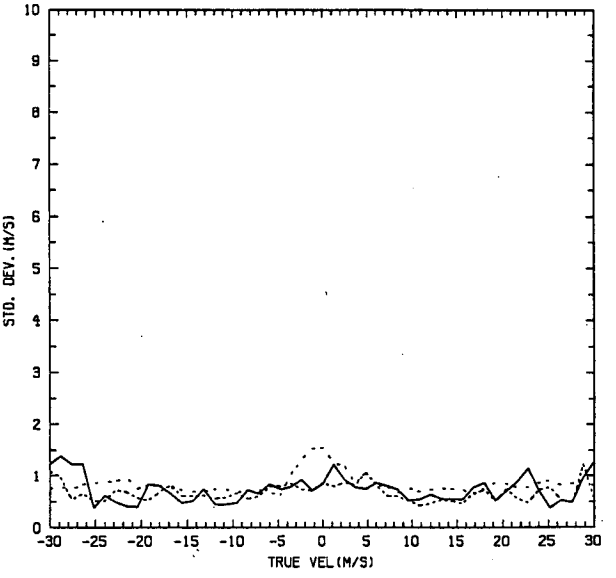

FIG. 3b. The standard deviation of the six scan average velocity estimates for the case of 30 dB clutter/signal.

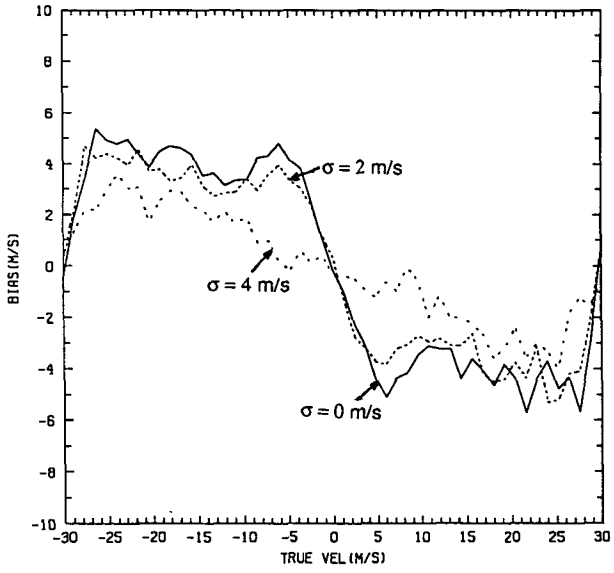

FIG. 4a. Like Fig. 3a but for a clutter/signal ratio of 40 dB.

nificant bias toward zero frequency at the 40 dB clutter/signal ratio where the effects of the clutter residue reverse the initial bias caused by the clutter filter.

5. Filter bank estimation

The second velocity estimation scheme makes explicit use of the fact that for this problem we are often more interested in high-velocity wind field features. Due to the nature of this requirement, we can afford a relatively large quantization step in the velocity estimates. In this processor, the target CPI which results from the FIR clutter filtering is then subjected to a bank of 20 narrow band FIR filters to produce a set of amplitudes A_j with one value for each filter in the following fashion:

$$A_j = |\sum_{k=1}^{M} f_j h_k^j|^2, \tag{5}$$

where the h_k^j are the (complex) filter impulse responses for the jth filter. Again trials are conducted for both 8- and 10-pulse target CPIs. The response functions of the filters peak at center frequencies which are spread uniformly across the Nyquist interval. Each output of the filter bank is subjected to a threshold procedure to remove those values which are due to the residue of the ground clutter. This thresholding process requires some a priori knowledge of the ground clutter amplitude. In an operational system, such information would come from a site specific map describing the regions of high-amplitude ground clutter. For this evaluation we have defined the threshold to be 7 dB above the mean ground clutter residue in the particular filter for the appropriate clutter amplitude. This threshold value was found to be a good compromise between lowering estimator bias and maximizing detection probability. Those cells which survive the thresholding procedure are then examined and the filter center velocity associated with the largest surviving A_j is output as the velocity estimate. Note that under some circumstances this technique will not produce an estimate at all since all of the filter amplitudes may fail the threshold testing. In this case, that estimate will not be used in the temporal averaging procedure. Plots of the bias, variance and the probability of making a measurement with this technique are shown in Figs. 5 and 6.

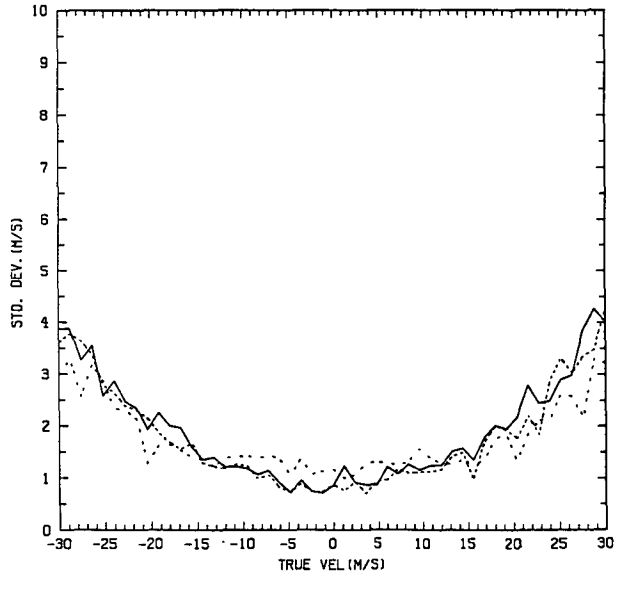

FIG. 4b. Like Fig. 3b but for a clutter/signal ratio of 40 dB.

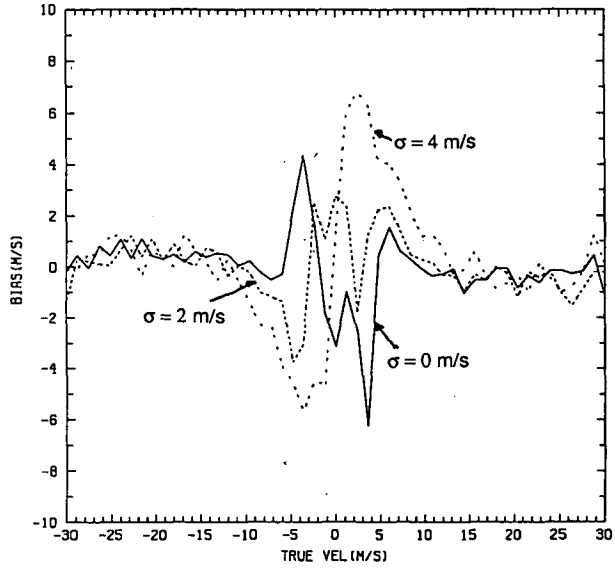

FIG. 5a. The arithmetic mean estimator bias for the clutter filter–filter bank processor system. This case is for a clutter/signal ratio of 40 dB.

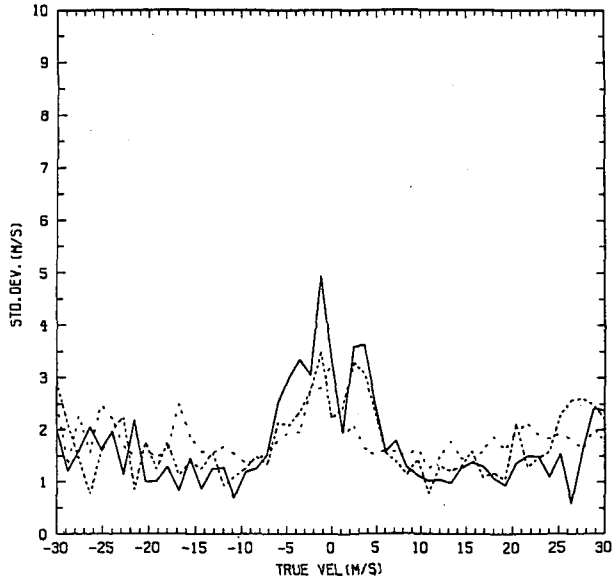

FIG. 5b. The standard deviation of the six scan average velocity estimates for the clutter filter–filter bank system. The clutter/signal ratio is 40 dB.

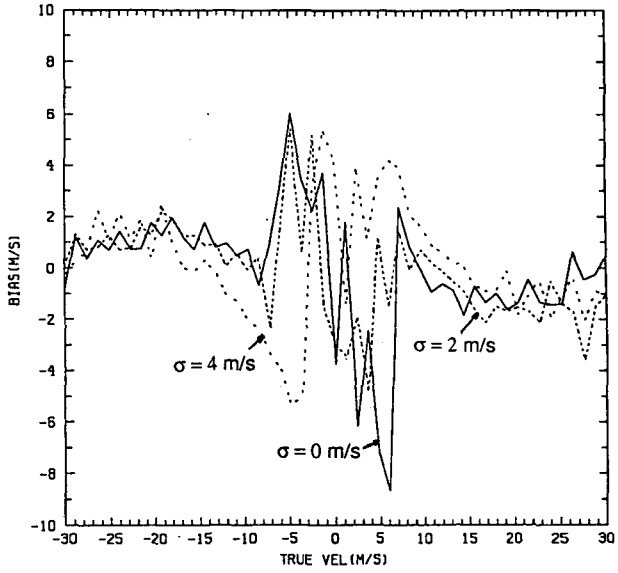

FIG. 6a. As in Fig. 5a but for 50 dB clutter/signal.

It can be seen from these results that as the clutter amplitude increases the range of low velocities where no detection can be made becomes wider, however detection of higher velocity weather remains possible even to clutter/signal ratios of 50 dB although with somewhat higher estimate error.

This ability to detect high-velocity weather signals is especially useful in light of our particular concern with microburst and severe wind shear events. The determination that an observation cannot be made is also useful so that an attempt may be made to use other scan observations of that resolution cell, or by using interclutter visibility techniques and spatial averaging over local regions to fill in small regions which are obscured by the presence of extreme amplitude clutter.

6. Summary and conclusions

In this paper we have presented a candidate architecture which seems suitable in some cases for the measurement of Doppler wind velocities using fast-

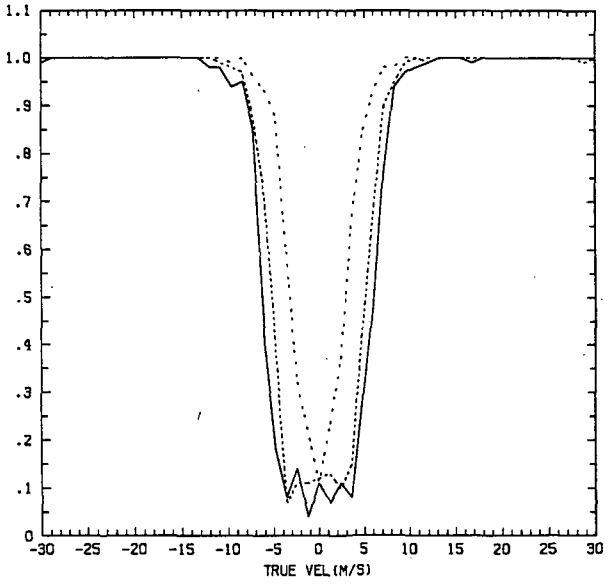

FIG. 5c. The measurement probability for the clutter filter–filter bank processor. The clutter/signal ratio is 40 dB.

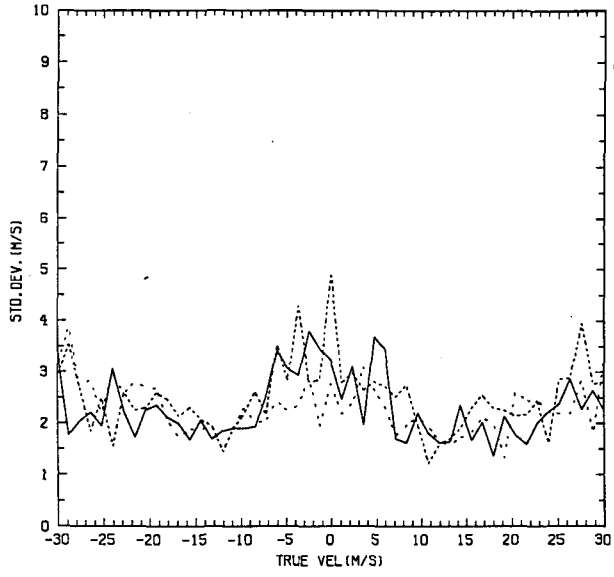

FIG. 6b. As in Fig. 5b but for 50 dB clutter/signal.

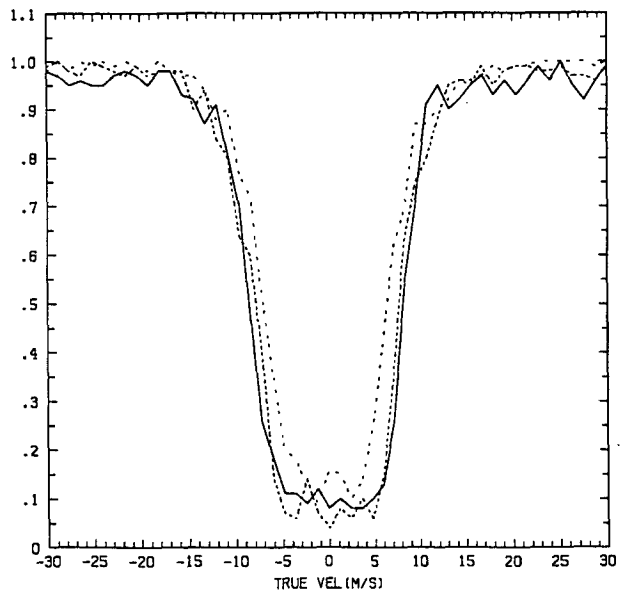

FIG. 6c. As in Fig. 5c but for 50 dB clutter/signal.

scanning radars. The technique consists of applying a finite-impluse response prefilter to the initial radar echo time series followed by the application of a velocity estimation scheme. This analysis considered the effects of the block-staggered radar waveform which is used by many modern airport surveillance radars. Measurements of the error characteristics of the velocity estimates for two different estimation techniques were performed for a variety of meteorological and clutter parameters.

In general, we found that both the pulse pair and the filter bank-based estimators are potentially capable of producing velocity estimates with bias and estimator standard deviations of order 2–3 m s^{-1} for medium and high Doppler velocities (greater than 6 m s^{-1}) and clutter/signal ratios to near 40 dB when used with a six-scan incoherent averaging processor. In addition, the filter bank-based estimators could make estimates of higher Doppler velocities in the presence of larger ground clutter echoes.

We view the outcome of this work as indicating that, as far as the signal processing techniques are concerned, it may be possible to provide a usable velocity measurement capability with fast-rotating sensors provided that the post-processing algorithms can operate with the lack of information regarding wind velocities less than about 6 m s^{-1}. In the particular case of the Airport Surveillance Radars, there are many other factors which must be considered, particularly the large vertical beamwidth. We are currently working on addressing some of these issues through the use of simulation studies. In addition, a field observation program is underway which will allow the performance of the observation system to be evaluated using recorded time series of actual radar-observed clutter and weather echoes.

Acknowledgments. The author wishes to thank M. L. Stone, J. E. Evans, and M. E. Weber of MIT-Lincoln Laboratory for their helpful comments. This work was sponsored by the Federal Aviation Administration. The United States Government assumes no liability for its contents or use thereof.

REFERENCES

Atlas, D., 1964: Advances in radar meteorology. *Adv. Geophys.*, **10,** 478 pp.

Doviak, R., and D. Zrnić, 1984: *Doppler Radar and Weather Observations.* Academic Press, 458 pp.

Hardesty, R. M., 1986: Performance of a discrete spectral peak frequency estimator for Doppler wind measurements. *IEEE Trans. Geosci. Remote Sens.*, **GE24.**

Oppenheim, A., and R. Schafer, 1975: *Digital Signal Processing.* Prentice-Hall, 585 pp.

Passarelli, R., and A. Siggia, 1981: The autocorrelation function and Doppler spectral moments. *Preprints, 20th Conf. on Radar Meteorology,* Boston, Amer. Meteor. Soc., 1981.

Shirakawa, M., and D. S. Zrnić: The probability density of a maximum likelihood mean frequency estimator. *IEEE Trans. on Accoust. Sp. and Sig. Proc.* ASSP-31 1197–1202.

Taylor, J. W., and G. Brunins, 1985: Design of a new airport surveillance radar. *Proc. IEEE,* Vol. 73.

Zrnić, D. S., 1975: Simulation of weatherlike Doppler spectra and signals. *J. Appl. Meteor.*, **14,** 619–620.